

Received 26 October 2023, accepted 4 November 2023, date of publication 7 November 2023,
date of current version 13 November 2023.

Digital Object Identifier 10.1109/ACCESS.2023.3330901

RESEARCH ARTICLE

A Hierarchical Approach for the Diagnosis of Sleep Disorders Using Convolutional Recurrent Neural Network

ADITYA WADICHAR¹, SHRUTI MURARKA¹, DHRUVI SHAH¹, ANKIT BHURANE¹,
MANISH SHARMA², HASAN S. MIR³, (Senior Member, IEEE),
AND U. RAJENDRA ACHARYA^{4,5,6}, (Senior Member, IEEE)

¹Department of Electronics and Communication Engineering, Visvesvaraya National Institute of Technology (VNIT), Nagpur 440010, India

²Department of Electrical and Computer Science Engineering, Institute of Infrastructure, Technology, Research and Management (IITRAM), Ahmedabad 380026, India

³Department of Electrical Engineering, American University of Sharjah, Sharjah, United Arab Emirates

⁴Department of Electronics and Computer Engineering, Ngee Ann Polytechnic, Singapore 599489

⁵Department of Bioinformatics and Medical Engineering, Asia University, Taichung 41354, Taiwan

⁶Department of Biomedical Engineering, School of Science and Technology, Singapore University of Social Sciences, Singapore 599491

Corresponding author: Shruti Murarka (shrutimurarka5@gmail.com)

ABSTRACT Sleep is an essential criterion for health. However, sleep disorders degrade the sleep quality. Hence, to diagnose sleep disorders, sleep monitoring is crucial. The cyclic alternating patterns (CAP) phases describe the sleep quality. However, CAP detection is a time-consuming, hectic, and uncertain process. Therefore, an automatic detection of CAP phases is necessary. This study proposes a hierarchical approach to identify sleep disorders and classify CAP phases. Single-channel EEG recording provided by the CAP sleep database has been utilized in this study. The proposed approach classifies CAP sequence into healthy or unhealthy. Further, it identifies sleep disorder of unhealthy sequence among periodic leg movement (PLM), rapid eye movement behaviour disorder (RBD), nocturnal frontal lobe epilepsy (NFLE), narcolepsy (NARCO), and insomnia (INS). Further using our prior work, the CAP phase of the sequence can be identified. The best model was obtained by long short-term memory (LSTM) along with convolutional neural network (CNN) for healthy-unhealthy, and disease classification with an accuracy of 91.45% and 90.55%, respectively. The same models gave an accuracy of 92.79% for healthy-unhealthy and 93.31% for disease classification when evaluated using dataset of only phase B, highlighting the importance of phase B for identifying sleep disorders.

INDEX TERMS Convolutional neural network (CNN), cyclic alternating patterns (CAP), deep learning, electroencephalogram (EEG), long short-term memory (LSTM), sleep disorders classification.

I. INTRODUCTION

Sleep is an important aspect of restoring and renewing human energy. Sufficient quality sleep is important for a healthy lifestyle. Sleep has been ignored for a long time, despite the fact that humans sleep for roughly 33% of their lives [1]. Obstructive rest apnea (OSA) and insomnia might lead to serious medical issues like obesity and strokes [2]. In the

United States of America, it is observed that 35% of adults have insomnia [3]. Not just in the United States of America, sleep disorders affect people throughout the world. Madrid-Valero et al. [4] investigated the prevalence of sleep problems in Spain and discovered that 38.2% of individuals had poor sleep quality. Similar worldwide research from 56 countries by Koyanagi and Stickley [5] found that the total prevalence of sleep disorders was 7.6%. The recent trend indicates that by 2030 this figure will rise to 260 million [6]. To minimize the figure, a reliable diagnostic method for a sleep disorder is required [7].

The associate editor coordinating the review of this manuscript and approving it for publication was Prakasam Periasamy.

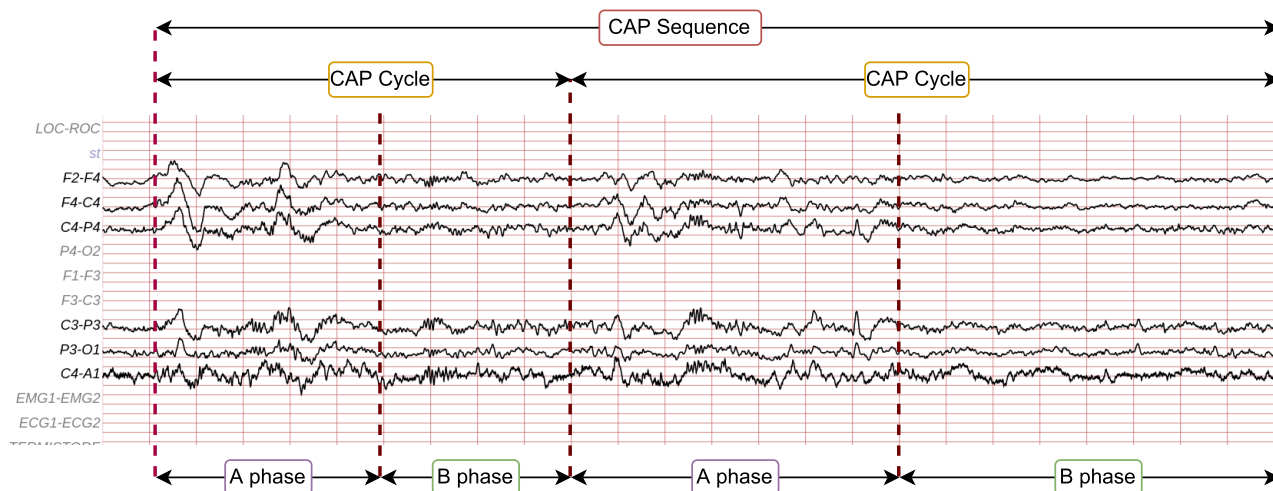


FIGURE 1. A CAP waveform example describing the phases, CAP cycle, and CAP sequence.

Subject polysomnogram (PSG) recordings are physiological signals recorded at night for sleep study and assessment. PSG is a multimodal signal, which means it is made up of distinct components such as electrooculogram (EOG), electroencephalogram (EEG), electromyogram (EMG), and electrocardiogram (ECG). When the PSG recordings are finished, the sleep stage is scored. A sleep expert typically analysis a PSG signal in a specific time, generally 30 seconds, and then estimates the sleep score based on numerous parameters [8], [9]. Visualizing PSG signals and manually assessing sleep stages is a time-consuming, costly, and demanding procedure requiring specialized knowledge. Furthermore, EEG signal variations are difficult to perceive visually due to their chaotic and unpredictable nature. As a result, experts are working on automatic detection and identification technologies to help them.

Sleep comprises non-rapid eye movements (NREM), a duration of inactivity, followed by rapid eye movements (REM), which are times of intense activity. Sleep is classified into five categories, according to the American Academy of Sleep Medicine (AASM) [10]: wakefulness (W), N1, N2, N3, and REM. NREM is composed of N1, N2, and N3. Numerous studies have explored sleep stages classification [11], [12], [13], [14], [15]. However, Sathapathy et al. [15] introduce an approach that combines CNN with LSTM, resulting in significantly improved accuracy.

A microstructure-based sleep scoring system was introduced in 2001 as an alternate way to define NREM sleep and incorporate phasic events such as delta bursts and K-complexes. This system is known as the cyclic alternating pattern (CAP) [16]. CAP is characterized by transient electrocortical events that occur at 1-minute intervals and differ from baseline electroencephalogram (EEG) activity. It consists of cyclic sequences of brain activity (phase A) followed by intervals of inactivation (phase B). A CAP cycle is defined as a phase A period followed by a phase B period,

and a CAP sequence consists of two or more CAP cycles. Fig 1 depicts phases A, B, and CAP cycle [16]. Several studies have been performed to classify CAP phases [17], [18], [19], [20], [21], [22], [23], [24], [25].

In this study, we considered sleep disorders like NFLE, INS, NARCO, RBD and PLM. NFLE is a neurological disorder induced by the frontal lobe and causes its patients to suffer from seizures, majorly affecting their lifestyles [26]. Symptoms of NFLE usually start showing within 30 minutes of falling asleep. It is challenging to diagnose NFLE as its symptoms are similar to that of psychiatric problems. Hence detecting NFLE using our proposed method can be very useful in diagnosing this disease. INS is widely described as either qualitative or quantitative discomfort with sleep. This is commonly associated with difficulties going asleep, staying asleep due to repeated awakenings or problems returning to sleep, and early morning awakenings [27]. The prevalence of insomnia in older adults is up to 75% [28]. Several studies have documented an increased risk of depression in older patients with persistent insomnia [29], [30]. Narcolepsy is defined by extreme tiredness and, cataplexy, and sleep-wake symptoms such as hallucinations, sleep disturbances, and sleep paralysis [31]. It is a rare neurological condition caused by the selective loss or malfunctioning of hypocretin (also known as orexin) neurons in the lateral. RBD is recognised by dream portrayal and a lack of muscular atonia while REM sleep [32]. In some cases, it can lead to major damage, forcing individuals to seek medical help, but in others, it is non-symptomatic and hence can be detected only during polysomnography. Periodic limb movement disorder is constantly jerking or cramping of the legs while in sleep. “Periodic” means that the leg movements are rhythmic, occurring every 20-40 seconds. PLM disorder disrupts sleep and also causes daytime sleepiness [33]. The sleep disorders discussed above directly affect sleep quality and an individual’s mental health. As the number of individuals

suffering from sleep disorders (such as PLM, insomnia, and narcolepsy) is multiplying, it is extremely critical to detect these difficulties by frequent sleep monitoring correctly.

The highlights of this work are:

- We propose a unified two-stage, 1-D CNN and LSTM-based approach for classifying healthy and unhealthy CAP signals.
- Our proposed model further identifies various sleep disorders, including insomnia, NFLE, RBD, narcolepsy, and PLM using CAP EEG signals'.
- The study is performed phase-wise using datasets of phase A and phase B individually and combined.
- The proposed approach does not require any pre/post-processing steps involved and only uses one channel's signal, minimizing its complexity for practical implementation.
- The incorporation of the LSTM layer in the model endows it with the capability to retain patterns within EEG signals, leading to enhanced accuracy compared to prior research.

In our knowledge, this is the first study to present a hierarchical strategy for the categorizing of both healthy and unhealthy (insomnia, nfle, rbd, narcolepsy, and plm) and CAP phases for all individuals. Also this is the first study to use the CAP sleep database to classify individuals as healthy or unhealthy and to use CAP data from an EEG signal (C4-A1) to diagnose sleep disorders. This study is the first to use sequential model on EEG signal leading significant improvement in accuracy of sleep disorder classification.

II. MATERIALS AND METHOD

A. DATA ACQUISITION

We have used publicly available polysomnographic recordings from the Sleep Disorder Center [16], [34]. The waveforms in the dataset include at least three EEG (electroencephalogram) channels (F3 or F4, O1 or O2, and C3 or C4), two EOG channels, respiration signals, bilateral anterior tibial EMG (electromyography), EKG (electrocardiogram) and EMG of the submental muscle. 16 subjects from 108 participants were free of neurological diseases and medicines that influence the central nervous system. The remaining 92 subjects include 40 subjects affected by NFLE disorder, 22 suffering from RBD disorder, 10 with PLM disorder, 9 with insomnia disorder, 5 from narcolepsy, 4 from SBD (sleep-disordered breathing), and 2 affected by bruxism.

Data from participants were obtained at various sampling rates, such as 512 Hz, 200 Hz, 128 Hz, and 100 Hz. For consistency, we have considered the participants whose data were collected at the rate of 512 Hz. We have considered only one channel, i.e., the C4-A1 or C3-A2 channel, out of many available channels in the dataset for simplicity and convenience. Only NREM sleep data was considered as CAP phases are insignificant in other stages. These recordings were segmented into two-second chunks. The summary of

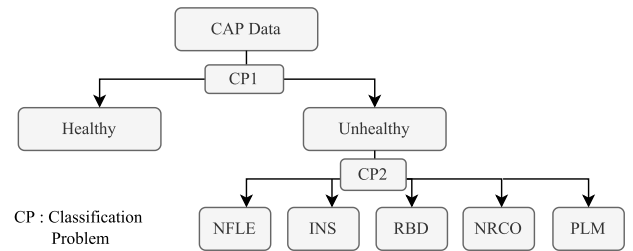


FIGURE 2. Stage-wise model for classification of sleep disorder and CAP phases.

the total number of samples available for each disorder after segmentation is given in Table 1.

To safeguard the precision of our classification and minimize the possibility of erroneously labeling unwell patients as healthy, our classification process is bifurcated into two sequential stages. The initial stage is dedicated to distinguishing between individuals in a healthy state and those with health concerns, while the subsequent stage categorizes individuals with sleep disorders into one of the five specific diagnostic categories. This two-stage approach ensures accurate classification and minimizes the risk of misclassification. We denote classification problems of healthy-unhealthy as CP1 and sleep disorder as CP2. For CP1, we consider disordered participants' data as unhealthy. The available data is severely unbalanced. To balance the data 1550 samples of each A1, A2 and A3 phases are considered for healthy subjects. Hence total of 4650 samples of phase A and equal samples of phase B were considered for a healthy dataset. The 930 samples of both phase A and phase B were considered for five disordered participants to balance the total samples of unhealthy data with healthy. Phase A of each disordered data consists of 310 samples of each A1, A2 and A3 phases. The summary of the dataset for CP1 is given in Table 2

Table 3 summarises the total number of samples used for CP2. Phase A2 of narcolepsy has the minimum number of samples available (table 1). Hence to balance the data 1593 samples of each sub-phases of A and 4779 samples of phase B are considered. The same method is followed for other disorders. This study did not consider SBD and bruxism disordered participants due to insufficient data.

B. PROPOSED APPROACH

Fig 2 shows the general hierarchical model of proposed approach. In the first stage, CP1 is performed by feeding an input segment is fed to proposed model (M1). If the sequence is predicted as unhealthy, in the next stage, CP2 is performed by feeding sequence to M1, identifying the sleep disorder corresponding to the input segment. Further another model (M2) performs the CAP phase classification irrespective of the health disorder as discussed in [17].

The extracted data for each model was split into training and test data according to a standard ratio of 80% and 20%, respectively. Further, 20% of the training data was

TABLE 1. Total number of samples available after segmentation.

Subjects		Phase A				Phase B	Total	
		A1	A2	A3	Total			
Healthy		4654	1551	2847	9052	62880		71862
Unhealthy	Insomnia	2932	1660	4162	8754	47055	55809	794922
	Narcolepsy	2958	1593	4255	8806	45330	54136	
	PLM	3990	2989	7670	14649	67080	81729	
	RBD	11230	7350	20620	39200	206805	246005	
	NFLE	25047	12596	23725	61368	295875	357243	
	Total	46157	26188	60432	132777	662145		
Total		50811	27739	63279	141829	725025		866854

TABLE 2. Total number of samples used for CP1 classification.

Subjects		Phase A	Phase B	Total	
Healthy		4650	4650		9300
Unhealthy	Insomnia	930	930	1860	9300
	Narcolepsy	930	930	1860	
	PLM	930	930	1860	
	RBD	930	930	1860	
	NFLE	930	930	1860	
	Total	4650	4650		
Total		9300	9300		18600

TABLE 3. Total number of samples considered for CP2 classification.

Subjects	Phase A	Phase B	Total
Insomnia	4779	4779	9558
Narcolepsy	4779	4779	9558
PLM	4779	4779	9558
RBD	4779	4779	9558
NFLE	4779	4779	9558
Total	23895	23895	47790

reserved for validation purposes. The training and validation data were initially utilized for determining layers of the model architecture and hyperparameter tuning. The models were trained until training was stopped by an early stopping callback [35]. This prevents the model from overfitting by stopping the training at a point where a model stops improving on the validation dataset. The hyperparameters were tuned to obtain the best possible performance using the validation dataset.

C. PROPOSED MODELS

Manual feature extraction from data is required for traditional classifiers. On the other hand, feed-forward neural network or artificial neural networks (ANNs) classifiers require many parameters to train and have a fuzzy architecture. A CNN eliminates the need for manual processing by automatically extracting features using various filters [36]. Furthermore in CNN, a kernel is convoluted with the whole signal, i.e., it shares kernel parameters, requiring fewer parameters to train and demanding less processing than traditional classifiers [37]. A recurrent neural network (RNN) is recognized for handling data from the present and the immediate past, acquiring memory and knowledge of context by thoroughly comprehending sequences [38]. To differentiate the morphological traits and temporal patterns for each sleep

condition from the EEG signal, we propose a convolutional recurrent neural network (CRNN). The convolutional layer's characteristics can be expressed by the equation (1) as,

$$v_k^l = b_k^l + \sum_{c=0}^{n_c-1} \sum_{j=0}^{n-1} w_{c,j}^l u_{c,k+j}^{l-1}$$

$$u_k^l = f(v_k^l) \quad (1)$$

where, superscript l and subscripts c, k denotes the layer, channel index and index position, respectively. The 1-D input signal and kernel are represented by U and W , respectively, while the output signal ($U * W$) is represented by V . The n_c and n variables represent the number of channels and kernel length, respectively. When the kernel passes over the input signals, each CNN layer's bias (b) and weights (W) are updated. The kernel creates feature maps after processing the input signals.

The output feature map (O) given by [39] the equation (2) as,

$$O_n^l = (U|_{W(i,j)})_n * (W(i,j))_n \quad (2)$$

where the elements of $(U|_{W(i,j)})_n$ represent the elements of U from n to the dimension of $W(i,j)$. The restricted matrix of the input matrix to the weight matrix is denoted by $(U|_{W(i,j)})_n$.

LSTM is a recurrent neural network and has better memorizing of specific patterns and also solves the problem of vanishing gradients [40]. Each LSTM unit or cell consists of the input gate, forget gate, and output gate. The equations for the forward pass of an LSTM cell can be given by equation (3),

$$f_t = \sigma(W_f[h_{t-1}, x_t] + b_f)$$

$$i_t = \sigma(W_i[h_{t-1}, x_t] + b_i)$$

$$o_t = \sigma(W_o[h_{t-1}, x_t] + b_o)$$

$$\tilde{c}_t = \tanh(W_c[h_{t-1}, x_t] + b_c)$$

$$c_t = f_t * c_{t-1} + i_t * \tilde{c}_t$$

$$h_t = o_t * \tanh(c_t) \quad (3)$$

where x_t is the input vector at the current instant and h_{t-1} is the hidden state at the last instant. The assigned weight, Wq , can have one of the following subscripts: i (input gate), f (forget gate), o (output gate), or c (cell state). Candidate values vector is represented by \tilde{c}_t and cell state vector by c_t , where t stands for the time step. The initial values of

TABLE 4. Architecture details of proposed 1D-CNN with LSTM based model for CP1 and CP2.

Sr. No.	Layer	Kernel Size	Total filters	Unit Size	Trainable Parameters	Output Shape
1	1D_Conv	7	32	-	256	(1024, 32)
2	1D_Conv	9	16	-	4624	(1024, 16)
3	1D_Conv	5	32	-	2592	(1024, 32)
4	ReLU	-	-	-	0	(1024,32)
5	LSTM	-	-	100	53200	(100)
6	Dense	-	-	1	101	(1)
6	Dense	-	-	5	505	(5)

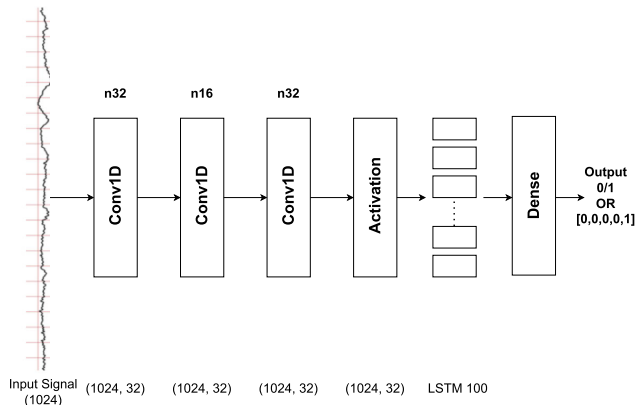


FIGURE 3. Visualisation of proposed 1-D CRNN model.

hidden state and cell state are $h_0 = 0$ and $c_0 = 0$. b denotes the biases for each of the gates, respectively. A forget gate eliminates information from the cell state. The input gate is responsible for updating the cell’s state with new information. The output gate is in charge of obtaining information from the present cell state. The sigmoid function ($\sigma()$) sets the activation vector values for each of the three gates to a value between 0 and 1. The value 1 signifies that the new/current information is important and should be retained, whereas the 0 value indicates that it should be discarded. The new information to be added in the cell state is stored in \tilde{c}_t using the tanh function, which outputs between -1 to 1. The cell state is updated using candidate values (\tilde{c}_t) and old cell state (c_{t-1}). The output h_t is a filtered version of the cell state.

The visualization of the proposed model M1 for CP1 and CP2 is shown in fig 3. The model extracts required features using three 1-D convolutional layers with stride one. Consider a 2-second input having 1024 samples. The network begins with a convolutional layer with 32 filters of kernel size 7, generating 32 feature maps of length 1024. The second layer comprises 16 filters with kernel size 9 that construct 16 feature maps of the same length using features retrieved by the previous layer. This set of features is then processed through a third convolutional layer with 32 filters with kernel size 5, yielding 32 feature maps of length 1024. Following the convolutional layers is the ReLU activation function. In our model, the LSTM layer consists of 100 units, which implies there will be 100 LSTM cell in parallel, and the output of this layer will have the same dimension as the number of units, which in this model is 100. The input given to the LSTM

TABLE 5. Details of hyperparameters in the proposed 1D-CRNN model.

Hyperparameters	
Optimizer	Adam
Beta1	0.9
Beta2	0.999
Learning rate	0.001
Epsilon	1e-07
Loss function	Binary crossentropy
Batch Size	100

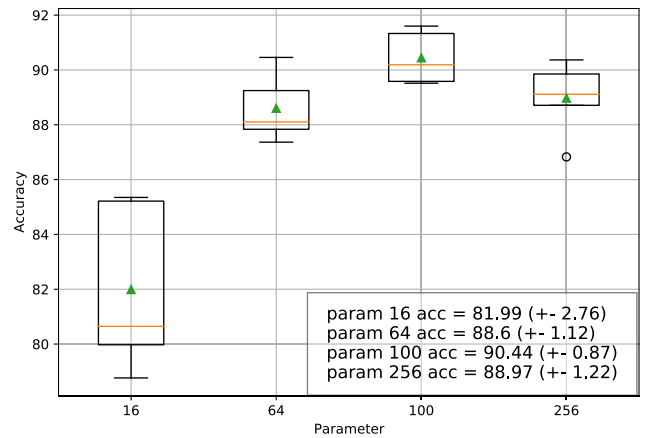
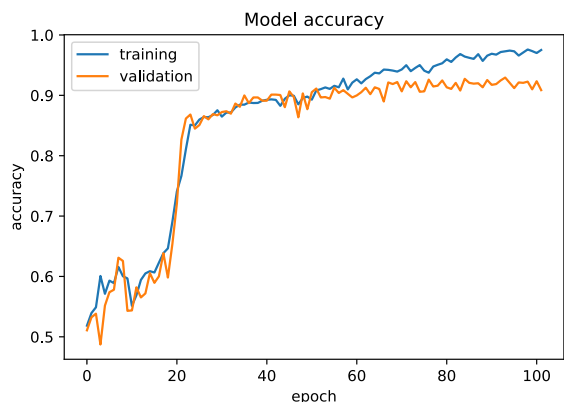


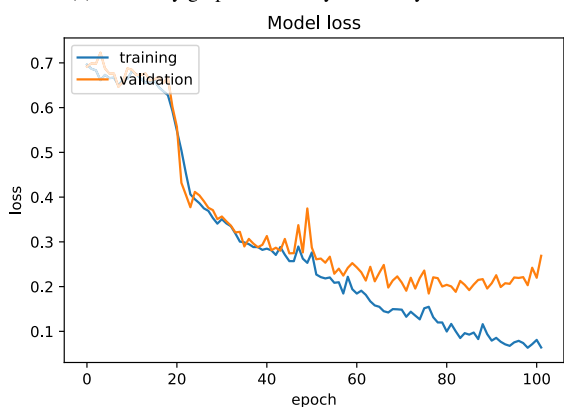
FIGURE 4. Hyperparameter optimization for the LSTM layer.

layer is a vector of size (1024, 32). Hence the timestamp (t) will take values from 1 to 1024. Thus at each instance, a vector of size 32 will be simultaneously passed through each LSTM unit, and there will be 1024 such instances. The feature maps are then condensed to a single column vector and classified with ultimately linked dense layers. This is then passed through the model’s final layer, a dense layer with five neurons and softmax activation for the CP2 and a single neuron with sigmoid activation for the CP1. The model may be holistically trained using just one loss function, although composed of two different types of neural networks. Tables 4 and 5 provides the details of the proposed model.

Dataset was generated from edf and txt files provided by Goldberger et al. [34] using MATLAB R2021a [41]. Google Colab [42] was used to train models which use the Google Compute Engine backend written in Python 3. It gives access to 13 GB RAM, 107.72 GB memory, and GPU. The proposed models were developed using Keras (v2.7.0) and Tensorflow (v2.7.0) backends which are python-based deep learning technologies. Training time for the CP1 is 45:38 mins, and for the CP2, it is 4:28:49 hrs.



(a) Accuracy graph for healthy-unhealthy classification



(b) Loss graph for healthy-unhealthy classification

FIGURE 5. Performance graphs for CP1 during training.

The number of layers and parameters of proposed model are tuned by brute force method. Fig 4 shows the model’s performance when the LSTM layer is adjusted to 16, 64, 100, and 256 for CP1. The mean and standard deviation of each parameter is shown using a box plot in fig 4. The parameter 100 has the highest classification accuracy with a low standard deviation compared to other considered parameters. Hence it is selected for the LSTM layer. With the change of parameters, the validation performance curve of the model is also updated continuously. Similarly, other layer parameters and hyperparameters are tuned, and the optimal model is selected that produces the best result. The final model and parameters obtained after hyperparameter optimization are given in Tables 4 and 5. The Adam optimizer having default values from Keras was used to optimize the model [43].

III. RESULTS

A. CP1

The proposed model achieved training, validation, and test accuracies of 97.51%, 90.86% and 91.45%, respectively. Fig 5 shows the accuracy graph and loss graph on training and validation dataset over the 100 epochs. Throughout the epochs, both training and validation losses exhibit a decreasing trend; however, a point is reached where the

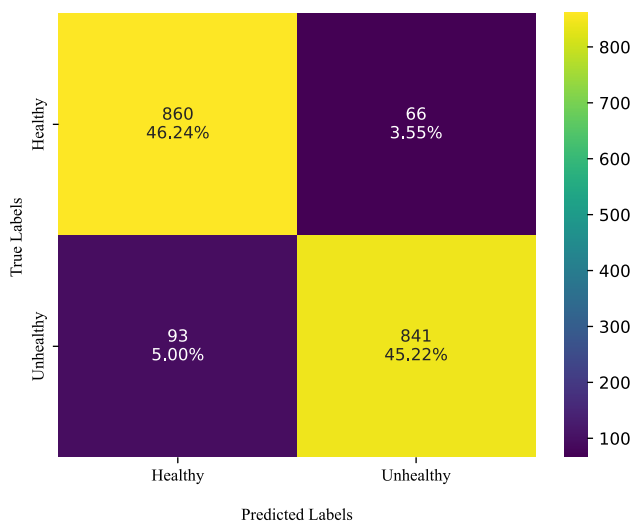


FIGURE 6. Confusion matrix for healthy-unhealthy classification.

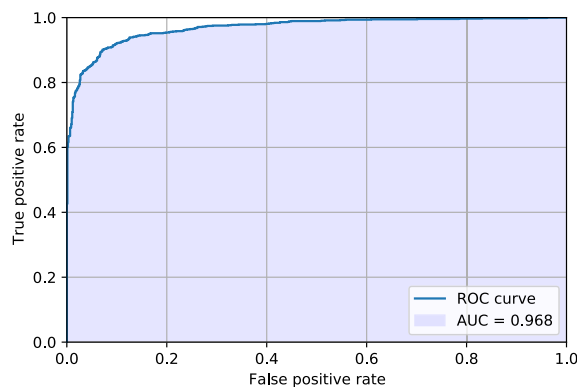


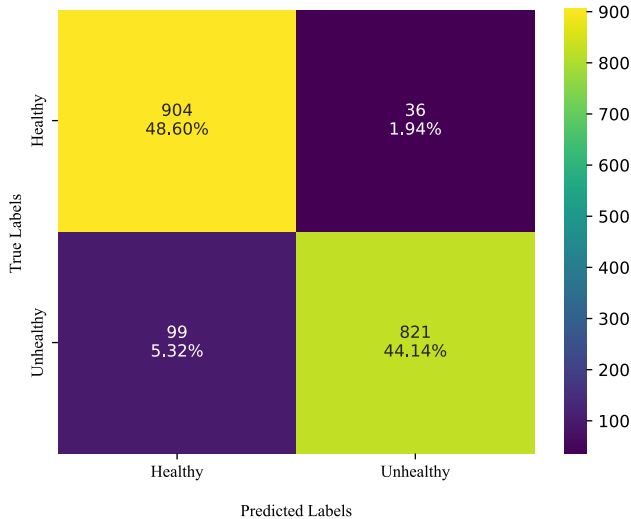
FIGURE 7. ROC for healthy-unhealthy classification model.

validation loss plateaus. To prevent overfitting, the decision was made to select the final model at the juncture where it ceased to exhibit improvements in terms of the validation loss. This strategy ensures that the model generalizes well without excessively fitting the training data. The confusion matrix for the proposed model is given in fig 6.

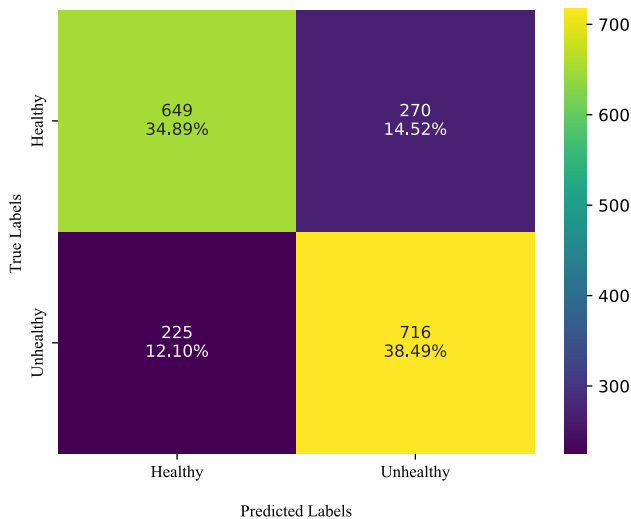
The sensitivity of the given model is its ability to accurately identify sick subjects, whereas specificity is its capacity to correctly identify healthy subjects [44]. The model’s precision is measured by its ability to refrain from categorizing healthy as unhealthy subjects [44]. The performance parameters for the proposed model and 10-fold cross-validation are summarised in Table 6. A probability curve called the receiver operator characteristic (ROC) compares the true positive rate (TPR) and false negative rate (FNR) at various threshold levels. The classifier’s ability to differentiate between classes is determined by the area under the curve (AUC) [45]. The ROC curve for the model is shown in Fig 7. The AUC was obtained as 0.9683. The 10-fold cross-validation performed on the proposed model using a dataset of both phases gave training, validation, and test accuracies as $(91.53 \pm 1.07)\%$, $(83.60 \pm 0.57)\%$ and $(83.94 \pm 0.99)\%$,

TABLE 6. Model accuracies and performance parameters for CP1 using 1D CNN + LSTM.

Dataset	Accuracy (%)			Performance parameters (%)				
	Train	Validation	Test	Precision	Specificity	Sensitivity	F1	AUC
Both phases	97.51	90.86	91.45	92.72	92.87	90.04	91.36	96.83
Phase B	96.53	93.34	92.79	95.79	96.17	89.23	92.40	97.51
Phase A	92.28	73.79	73.38	72.61	70.62	76.08	74.31	80.08



(a) Classification using phase B



(b) Classification using phase A

FIGURE 8. Confusion matrix for healthy-unhealthy classification using dataset of B & A phases.

respectively. While Precision, Specificity, Sensitivity, F1 and AUC were obtained as (85.35±1.27), (85.90±1.51), (81.98±1.90), (83.61±1.08) and (92.16±0.95), respectively.

The study is further extended to evaluate the model using data consisting of samples of only one phase, i.e. either phase A or phase B. The same model architecture has been used to train and evaluate both models. Fig 8(a) shows the confusion matrix for the dataset of phase B and fig 8(b) shows the confusion matrix for dataset of phase A. For data

TABLE 7. Model accuracies for CP2 using 1D-CNN + LSTM.

Dataset	Accuracy (%)		
	Train	Validation	Test
Both phases	93.21	89.83	90.55
Phase B	97.03	94.18	93.31
Phase A	76.34	68.44	67.77

TABLE 8. Performance parameters for CP2 using hold-out validation.

Subject	Recall (%)	Precision (%)	F1-score (%)
RBD	96.41%	90.32%	93.26%
NFLE	91.01%	93.55%	92.26%
Narcolepsy	89.14%	91.56%	90.33%
Insomnia	89.47%	91.02%	90.23%
PLM	86.70%	86.52%	86.61%

TABLE 9. Performance parameters for CP2 for 10-fold cross-validation.

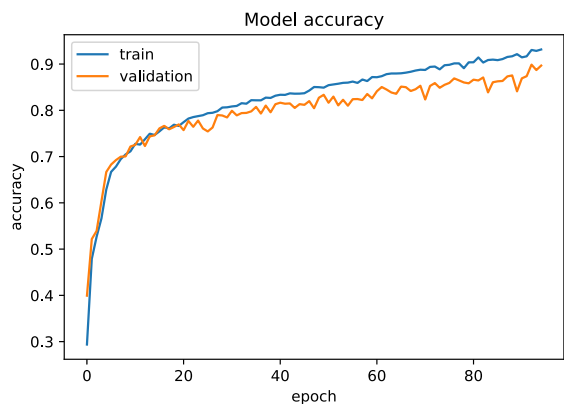
Subject	Recall (%)	Precision (%)	F1-score (%)
RBD	78.8 ± 4.26	77.1 ± 3.23	77.8 ± 2.13
NFLE	83.4 ± 3.26	81.2 ± 3.84	82 ± 1.26
Narcolepsy	81 ± 3.34	83.7 ± 2.14	82.1 ± 1.92
Insomnia	82.7 ± 2.32	86.9 ± 3.04	84.8 ± 0.97
PLM	89.4 ± 2.33	87.4 ± 2.33	88.4 ± 1.28

with phase A, the model gave training accuracy of 92.28% and validation accuracy of 73.73%. When the model was evaluated on 1860 test samples, we obtained test accuracy of 73.38%. While for the data with phase B, a training accuracy of 96.53%, validation accuracy of 91.34% and test accuracy of 92.79% were obtained. The comparison of these three models is shown in table 6. The significantly higher accuracy for data with phase B compared to data with phase A signifies that distinctive features required to predict diseases are higher in phase B than in phase A.

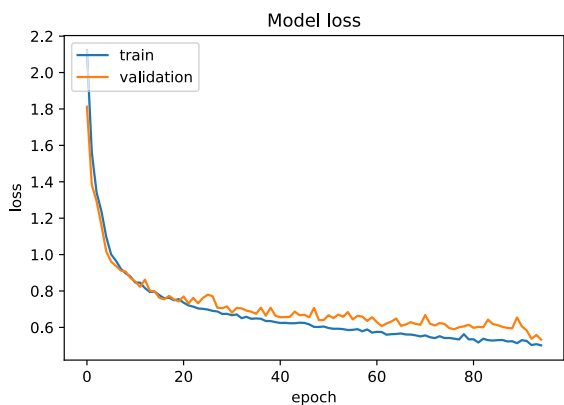
B. CP2

80% of the dataset was used for training, and the remaining 20% was used for testing the model. 20% of the training dataset was utilized for validation purpose. The performance was evaluated for different architectures, namely 1D-CNN, 1D-CNN with skip connections, LSTM, and convolutional recurrent neural network (CRNN). Table 7 summarizes different accuracies of proposed model.

The best model obtained a training accuracy of 93.21% and validation accuracy of 89.83%. Fig 9 shows the accuracy, training dataset loss and validation dataset loss while the model was being trained. The loss of training and validation dataset are very close to each other implying the model is not overfitted. This model was then evaluated on test dataset



(a) Accuracy graph for disease detection



(b) Loss graph for disease detection

FIGURE 9. Performance graphs during training for disease dataset.



FIGURE 10. Confusion matrix for disease classification using dataset of both phases.

consist of 9558 samples to get an overall accuracy of 90.55%. Fig 10 shows the confusion matrix for the proposed model.

Table 8 summarises the precision, recall and f1-score of the proposed model. The f1-score for insomnia, nfle, narcolepsy, rbd and plm are 90.23%, 92.26%, 90.33%, 93.26% and 86.61%, respectively. The high values of f1-score indicate the model’s ability to correctly distinguish between sleep disorders. The 10-fold cross-validation has been performed



FIGURE 11. Confusion matrix for disease classification using dataset of B phase.

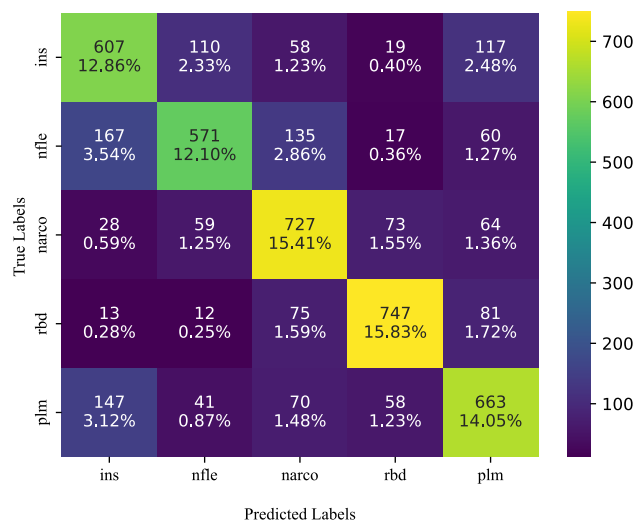


FIGURE 12. Confusion matrix for disease classification using dataset of A phase.

on the proposed model using dataset including both phases which gave training, validation and test accuracies as $(91.11 \pm 0.82)\%$, $(83.12 \pm 1.08)\%$ and $(83.05 \pm 1.19)\%$, respectively.

The study is further extended to evaluate the model using data consisting of samples of only one phase, i.e. either phase A or phase B. The same model architecture has been used to train and evaluate all models. The confusion matrix for disease classification using phase B data is shown in Fig 11 and the confusion matrix for phase A data is shown in fig 12. For phase B data, the model gave a test accuracy of 93.31% while for phase A data, the model gave test accuracy of 67.77%. The comparison of the three models is shown in table 7.

IV. DISCUSSION

Efficient sleep analysis is a critical aspect of diagnosing sleep disorders. Dimitriadis et al. [8] employed EEG data for sleep problem detection using a random forest model

TABLE 10. Comparison of studies on sleep disorders classification.

Study	Features	Classifier	Signal	Disorders	Accuracy
Dimitriadis et al. [8]	Cross-frequency coupling (CFC)	random forest (RF)	EEG (non-CAP)	Healthy, BRUX, SBD, INS, SBD, NARCO, NFLE, PLM, RBD	74%
Sharma et al. [46]	Hjorth parameters	EBTC	EMG + EOG	Healthy, INS, NFLE, Narco, RBD, PLM	87.5%
Sharma et al. [47]	Norm features	KNN and SVM	ECG	INS	97.87%
Kumar et al. [48]	-	CNN	ECG	INS	98.91%
Sharma et al. [49]	Optimal bi-orthogonal filter bank	Ensemble of bagged trees	EEG (C4-A1)	Healthy and INS	95.60%
Widasari et al. [50]	Spectral features and sleep quality parameters	Ensemble of bagged trees	ECG	Healthy, INS, RBD and SDB	86.27%
Sharma et al. [51]	Hjorth parameters	Ensemble Bagged trees	EEG (C4-A1), (CAP + non-CAP)	Healthy, INS, NFLE, NARCO, RBD, SDB, PLM	82.0%
Proposed work	-	LSTM+CNN	EEG (C4-A1)	Healthy and Unhealthy INS, NFLE, NARCO, RBD, PLM	91.45% 90.55%

in a recent research. However, they have used a non-CAP dataset. Recently, Erdenebayar Urtnasan et al. [52] suggested a sleep disorder network based on a convolutional neural network for ECG input. Reference [47] have used optimal antisymmetric biorthogonal wavelet filter bank and [48] have used scalogram with CNN on ECG signals. However they have only identified the insomnia disorder. In a different recent investigation, Sharma et al. [51] introduced a methodology for the automated differentiation of both healthy and six sleep disorder signals using EEG data from two channels. Their approach utilized the optimal triplet half-band filter bank (THFB) for feature extraction and relied on supervised machine learning algorithms for the classification task. However, it's worth noting that the F1 score for the healthy class was observed to be 83%, suggesting a relatively higher likelihood of misclassification between individuals classified as healthy and those with health concerns. The paper [53] provides an extensive comparison of various studies related to automated sleep disorder classification. The studies utilizing the CAP dataset are briefly compared in Table 10.

In this work, we propose a unified and multistage hierarchical approach to diagnose the CAP sleep disorders of a patient and identify the CAP phase using EEG recordings having CAP phases. In the first stage, the proposed model classifies a CAP sequence into healthy and unhealthy with a classification accuracy of 91.45%. At the next stage, the same model diagnoses the unhealthy CAP sequence into various sleep disorders with a classification accuracy of 93.21%. When model M1 was evaluated using a single-phase dataset for CP1, the model performed better for the phase B dataset with an accuracy of 92.7%. A similar observation was made when the model M1 was evaluated for CP2, which performed

better on the phase B dataset with an accuracy of 93.3%. The significantly higher accuracy for data with phase B compared to data with phase A signifies that distinctive features required to predict diseases are higher in phase B than in phase A.

Conventional machine learning models rely on features extracted from PSG recordings, and overfitting is likely when training on high-dimensional PSG records [54], [55]. However, when PSG recordings are translated to a feature vector with a lower dimension [54], feature extraction may cause information loss. Furthermore, the features must be manually retrieved, which is a cumbersome and subjective task [56]. As a result, by reducing the need for feature extraction, our proposed model successfully solved these constraints.

Our study's primary characteristics and advantages are as follows:

- All models are trained using single channel EEG signal with balanced data to obtain unbiased and robust categorization.
- The model comprises an LSTM layer, allowing it to recognize and retain patterns within EEG signals.
- The proposed model requires no pre/post-processing stages and has end-to-end architecture.
- The study is performed using the dataset of phase A and phase B individually as well as combined.

However, this study is performed on dataset collected from one sleep disorder centre in Italy. The study can be expanded by evaluating the models on more datasets collected from different regions. In the future, the exploration of more advanced DL algorithms for intricate feature extraction, enhancing model accuracy is a compelling avenue. Furthermore, the integration of these models with development libraries to

create intuitive user interfaces for medical professionals shows significant promise.

V. CONCLUSION

This work proposes a hierarchical approach to identifying a given EEG signal's sleep disorder and CAP phase. Model in the first stage of hierarchy classifies input signals into healthy or unhealthy participants (CP1). The next stage classifies unhealthy subjects into five different sleep disorders (CP2), namely insomnia, NFLE, narcolepsy, RBD, and PLM. We evaluated the proposed model on a balanced dataset to train models, i.e., the dataset contained an equal number of samples of each class and equal samples of phase A and phase B in every class. The proposed model achieved the highest classification accuracy of 91.45% using the dataset of both phases, 92.79% using the dataset of phase B only, and 73.38% using the dataset of phase A only for CP1. While for CP2, the proposed model obtained the highest accuracy of 90.55% using the dataset of both phases, 93.31% using the dataset of only the B phase, and 67.77% using the dataset of only the A phase. For both the cases, higher accuracy is obtained for phase B only based classification. It indicates that the B phases, generally intervals of inactivation, contain more distinctive features to identify sleep disorders. The proposed approach can be a helpful tool for medical professionals in categorizing CAP phases and diagnosing sleep disorders.

ACKNOWLEDGMENT

(Aditya Wadichar, Shruti Murarka, and Dhruvi Shah contributed equally to this work.)

REFERENCES

- [1] J. W. Cho and J. F. Duffy, "Sleep, sleep disorders, and sexual dysfunction," *World J. Men's Health*, vol. 37, no. 3, p. 261, 2019.
- [2] E. J. W. Van Someren, "Brain mechanisms of insomnia: New perspectives on causes and consequences," *Physiol. Rev.*, vol. 101, no. 3, pp. 995–1046, Jul. 2021.
- [3] S. X. Zhang, K. Batra, W. Xu, T. Liu, R. K. Dong, A. Yin, A. Y. Delios, B. Z. Chen, R. Z. Chen, S. Miller, X. Wan, W. Ye, and J. Chen, "Mental disorder symptoms during the COVID-19 pandemic in Latin America—A systematic review and meta-analysis," *Epidemiol. Psychiatric Sci.*, vol. 31, p. e23, Apr. 2022.
- [4] J. J. Madrid-Valero, J. M. Martínez-Selva, B. R. do Couto, J. F. Sánchez-Romera, and J. R. Ordoñana, "Age and gender effects on the prevalence of poor sleep quality in the adult population," *Gaceta Sanitaria*, vol. 31, no. 1, pp. 18–22, Jan. 2017.
- [5] A. Koyanagi and A. Stickley, "The association between sleep problems and psychotic symptoms in the general population: A global perspective," *Sleep*, vol. 38, no. 12, pp. 1875–1885, Dec. 2015, doi: 10.5665/sleep.5232.
- [6] H. W. Loh, C. P. Ooi, J. Vinesh, S. L. Oh, O. Faust, A. Gertych, and U. R. Acharya, "Automated detection of sleep stages using deep learning techniques: A systematic review of the last decade (2010–2020)," *Appl. Sci.*, vol. 10, no. 24, p. 8963, Dec. 2020. [Online]. Available: <https://www.mdpi.com/2076-3417/10/24/8963>
- [7] V. Kapur, K. P. Strohl, S. Redline, C. Iber, G. O'Connor, and J. Nieto, "Underdiagnosis of sleep apnea syndrome in U.S. communities," *Sleep Breathing*, vol. 6, no. 2, pp. 49–54, 2002.
- [8] S. Dimitriadis, C. Salis, and D. Liparas, "An automatic sleep disorder detection based on EEG cross—Frequency coupling and random forest model," *J. Neural Eng.*, vol. 18, Mar. 2021, Art. no. 046064.
- [9] J. Rodríguez-Sotelo, A. Osorio-Forero, A. Jiménez-Rodríguez, D. Cuesta-Frau, E. Cirugeda-Roldán, and D. Peluffo, "Automatic sleep stages classification using EEG entropy features and unsupervised pattern analysis techniques," *Entropy*, vol. 16, no. 12, pp. 6573–6589, Dec. 2014. [Online]. Available: <https://www.mdpi.com/1099-4300/16/12/6573>
- [10] R. Berry, R. Brooks, C. Gamaldo, S. Harding, R. Lloyd, C. Marcus, and B. Vaughn. (1999). *The AASM Manual for the Scoring of Sleep and Associated Events: Rules, Terminology and Technical Specifications*. [Online]. Available: <https://aasm.org/>
- [11] E. Eldele, Z. Chen, C. Liu, M. Wu, C.-K. Kwok, X. Li, and C. Guan, "An attention-based deep learning approach for sleep stage classification with single-channel EEG," *IEEE Trans. Neural Syst. Rehabil. Eng.*, vol. 29, pp. 809–818, 2021.
- [12] E. Khalili and B. M. Asl, "Automatic sleep stage classification using temporal convolutional neural network and new data augmentation technique from raw single-channel EEG," *Comput. Methods Programs Biomed.*, vol. 204, Jun. 2021, Art. no. 106063.
- [13] M. Sharma, D. Goyal, P. V. Achuth, and U. R. Acharya, "An accurate sleep stages classification system using a new class of optimally time-frequency localized three-band wavelet filter bank," *Comput. Biol. Med.*, vol. 98, pp. 58–75, Jul. 2018.
- [14] M. Sharma, S. Patel, S. Choudhary, and U. R. Acharya, "Automated detection of sleep stages using energy-localized orthogonal wavelet filter banks," *Arabian J. Sci. Eng.*, vol. 45, no. 4, pp. 2531–2544, Apr. 2020.
- [15] S. K. Satapathy, K. Shah, S. Shah, B. Shah, and A. Panchal, "A deep neural model CNN-LSTM network for automated sleep staging based on a single-channel EEG signal," in *Soft Computing for Problem Solving*, M. Thakur, S. Agnihotri, B. S. Rajpurohit, M. Pant, K. Deep, and A. K. Nagar, Eds. Singapore: Springer, 2023, pp. 55–71.
- [16] M. G. Terzano, L. Parrino, A. Sherieri, R. Chervin, S. Chokroverty, C. Guilleminault, M. Hirshkowitz, M. Mahowald, H. Moldofsky, A. Rosa, R. Thomas, and A. Walters, "Atlas, rules, and recording techniques for the scoring of cyclic alternating pattern (CAP) in human sleep," *Sleep Med.*, vol. 2, no. 6, pp. 537–553, Nov. 2001. [Online]. Available: <https://www.sciencedirect.com/science/article/pii/S1389945701001496>
- [17] S. Murarka, A. Wadichar, A. Bhurane, M. Sharma, and U. R. Acharya, "Automated classification of cyclic alternating pattern sleep phases in healthy and sleep-disordered subjects using convolutional neural network," *Comput. Biol. Med.*, vol. 146, Jul. 2022, Art. no. 105594. [Online]. Available: <https://www.sciencedirect.com/science/article/pii/S0010482522003869>
- [18] M. Sharma, A. A. Bhurane, and U. R. Acharya, "An expert system for automated classification of phases in cyclic alternating patterns of sleep using optimal wavelet-based entropy features," *Expert Syst.*, vol. 146, Feb. 2022, Art. no. e12939, doi: 10.1111/exsy.12939.
- [19] M. Sharma, V. Patel, J. Tiwari, and U. R. Acharya, "Automated characterization of cyclic alternating pattern using wavelet-based features and ensemble learning techniques with EEG signals," *Diagnosics*, vol. 11, no. 8, p. 1380, Jul. 2021. [Online]. Available: <https://www.mdpi.com/2075-4418/11/8/1380>
- [20] F. Mendonça, A. Fred, S. S. Mostafa, F. Morgado-Dias, and A. G. Ravelo-García, "Automatic detection of cyclic alternating pattern," *Neural Comput. Appl.*, vol. 34, no. 13, pp. 11097–11107, Jul. 2022.
- [21] H. W. Loh, C. P. Ooi, S. G. Dhok, M. Sharma, A. A. Bhurane, and U. R. Acharya, "Automated detection of cyclic alternating pattern and classification of sleep stages using deep neural network," *Int. J. Speech Technol.*, vol. 52, no. 3, pp. 2903–2917, Feb. 2022.
- [22] R. Largo, M. C. Lopes, K. Spruyt, C. Guilleminault, Y. P. Wang, and A. C. Rosa, "Visual and automatic classification of the cyclic alternating pattern in electroencephalography during sleep," *Brazilian J. Med. Biol. Res.*, vol. 52, no. 3, 2019, Art. no. e8059, doi: 10.1590/1414-431x20188059.
- [23] M. Sharma, H. Lodhi, R. Yadav, H. Elphick, and U. R. Acharya, "Computerized detection of cyclic alternating patterns of sleep: A new paradigm, future scope and challenges," *Comput. Methods Programs Biomed.*, vol. 235, Jun. 2023, Art. no. 107471. [Online]. Available: <https://www.sciencedirect.com/science/article/pii/S0169260723001372>
- [24] M. Sharma, S. Verma, D. Anand, V. M. Gadre, and U. R. Acharya, "CAPSCNet: A novel scattering network for automated identification of phasic cyclic alternating patterns of human sleep using multivariate EEG signals," *Comput. Biol. Med.*, vol. 164, Sep. 2023, Art. no. 107259. [Online]. Available: <https://www.sciencedirect.com/science/article/pii/S0010482523007242>

- [25] J. You, Y. Ma, and Y. Wang, "GTransU-CAP: Automatic labeling for cyclic alternating patterns in sleep EEG using gated transformer-based U-Net framework," *Comput. Biol. Med.*, vol. 147, Aug. 2022, Art. no. 105804.
- [26] S. Kansagra, "Sleep disorders in adolescents," *Pediatrics*, vol. 145, no. 2, pp. S204–S209, 2020.
- [27] D. Riemann, F. Benz, R. J. Dressle, C. A. Espie, A. F. Johann, T. F. Blanken, J. Leerssen, R. Wassing, A. L. Henry, S. D. Kyle, K. Spiegelhalter, and E. J. W. Van Someren, "Insomnia disorder: State of the science and challenges for the future," *J. Sleep Res.*, vol. 31, no. 4, Aug. 2022, Art. no. e13604.
- [28] V. Nguyen, T. George, and G. S. Brewster, "Insomnia in older adults," *Current Geriatrics Rep.*, vol. 8, pp. 271–290, Dec. 2019.
- [29] M. R. Irwin, C. Carrillo, N. Sadeghi, M. F. Bjurstrom, E. C. Breen, and R. Olmstead, "Prevention of incident and recurrent major depression in older adults with insomnia: A randomized clinical trial," *JAMA Psychiatry*, vol. 79, no. 1, pp. 33–41, 2022.
- [30] M. Liu, T. Hou, M. Nkimbeng, Y. Li, J. L. Taylor, X. Sun, S. Tang, and S. L. Szanton, "Associations between symptoms of pain, insomnia and depression, and frailty in older adults: A cross-sectional analysis of a cohort study," *Int. J. Nursing Stud.*, vol. 117, May 2021, Art. no. 103873.
- [31] C. L. Bassetti, A. Adamantidis, D. Burdakov, F. Han, S. Gay, U. Kallweit, R. Khatami, F. Koning, B. R. Kornum, and G. J. Lammers, "Narcolepsy-clinical spectrum, aetiopathophysiology, diagnosis and treatment," *Nature Rev. Neurol.*, vol. 15, no. 9, pp. 519–539, 2019.
- [32] E. Matar, S. J. McCarter, E. K. St Louis, and S. J. G. Lewis, "Current concepts and controversies in the management of REM sleep behavior disorder," *Neurotherapeutics*, vol. 18, no. 1, pp. 107–123, Jan. 2021.
- [33] G. Maiolino, V. Bisogni, D. Soranna, M. F. Pengo, G. Pucci, R. Vettor, C. Fava, G. L. Colussi, G. Bilo, C. Lombardi, G. Parati, G. P. Rossi, and A. Silvani, "Effects of insomnia and restless legs syndrome on sleep arterial blood pressure: A systematic review and meta-analysis," *Sleep Med. Rev.*, vol. 59, Oct. 2021, Art. no. 101497.
- [34] A. L. Goldberger, L. A. N. Amaral, L. Glass, J. M. Hausdorff, P. C. Ivanov, R. G. Mark, J. E. Mietus, G. B. Moody, C.-K. Peng, and H. E. Stanley, "PhysioBank, PhysioToolkit, and PhysioNet," *Circulation*, vol. 101, no. 23, pp. e215–e220, Jun. 2000, doi: 10.1161/01.cir.101.23.e215.
- [35] R. Heckel and F. F. Yilmaz, "Early stopping in deep networks: Double descent and how to eliminate it," 2020, *arXiv:2007.10099*.
- [36] K. Barrera-Llana, J. Burriel-Valencia, Á. Sapena-Bañó, and J. Martínez-Román, "A comparative analysis of deep learning convolutional neural network architectures for fault diagnosis of broken rotor bars in induction motors," *Sensors*, vol. 23, no. 19, p. 8196, Sep. 2023.
- [37] S. Albawi, T. A. Mohammed, and S. Al-Zawi, "Understanding of a convolutional neural network," in *Proc. Int. Conf. Eng. Technol. (ICET)*, Aug. 2017, pp. 1–6.
- [38] Y. Ensafi, S. H. Amin, G. Zhang, and B. Shah, "Time-series forecasting of seasonal items sales using machine learning—A comparative analysis," *Int. J. Inf. Manage. Data Insights*, vol. 2, no. 1, Apr. 2022, Art. no. 100058.
- [39] O. Yildirim, U. Baloglu, and U. Acharya, "A deep learning model for automated sleep stages classification using PSG signals," *Int. J. Environ. Res. Public Health*, vol. 16, no. 4, p. 599, Feb. 2019.
- [40] S. Hochreiter and J. Schmidhuber, "Long short-term memory," *Neural Comput.*, vol. 9, no. 8, pp. 1735–1780, Nov. 1997.
- [41] *MATLAB, Version 9.10.0.1602886 (R2021a)*, MathWorks Inc., Natick, MA, USA, 2021.
- [42] E. Bisong, *Building Machine Learning and Deep Learning Models on Google Cloud Platform: A Comprehensive Guide for Beginners*. Natick, MA, USA: The MathWorks Inc, Jan. 2019.
- [43] F. Chollet. (2015). *Keras*. [Online]. Available: <https://keras.io>
- [44] M. Sokolova and G. Lapalme, "A systematic analysis of performance measures for classification tasks," *Inf. Process. Manage.*, vol. 45, no. 4, pp. 427–437, Jul. 2009. [Online]. Available: <https://www.sciencedirect.com/science/article/pii/S0306457309000259>
- [45] C. X. Ling, J. Huang, and H. Zhang, "AUC: A statistically consistent and more discriminating measure than accuracy," in *Proc. IJCAI*, vol. 3, 2003, pp. 519–524.
- [46] M. Sharma, J. Darji, M. Thakrar, and U. R. Acharya, "Automated identification of sleep disorders using wavelet-based features extracted from electrooculogram and electromyogram signals," *Comput. Biol. Med.*, vol. 143, Apr. 2022, Art. no. 105224. [Online]. Available: <https://www.sciencedirect.com/science/article/pii/S0010482522000166>
- [47] M. Sharma, H. S. Dhiman, and U. R. Acharya, "Automatic identification of insomnia using optimal antisymmetric biorthogonal wavelet filter bank with ECG signals," *Comput. Biol. Med.*, vol. 131, Apr. 2021, Art. no. 104246.
- [48] K. Kumar, K. Gupta, M. Sharma, V. Bajaj, and U. Rajendra Acharya, "INSOMNet: Automated insomnia detection using scalogram and deep neural networks with ECG signals," *Med. Eng. Phys.*, vol. 119, Sep. 2023, Art. no. 104028. [Online]. Available: <https://www.sciencedirect.com/science/article/pii/S1350453323000838>
- [49] M. Sharma, V. Patel, and U. R. Acharya, "Automated identification of insomnia using optimal bi-orthogonal wavelet transform technique with single-channel EEG signals," *Knowl.-Based Syst.*, vol. 224, Jul. 2021, Art. no. 107078. [Online]. Available: <https://www.sciencedirect.com/science/article/pii/S0950705121003415>
- [50] E. R. Widasari, K. Tanno, and H. Tamura, "Automatic sleep disorders classification using ensemble of bagged tree based on sleep quality features," *Electronics*, vol. 9, no. 3, p. 512, Mar. 2020.
- [51] M. Sharma, J. Tiwari, V. Patel, and U. R. Acharya, "Automated identification of sleep disorder types using triplet half-band filter and ensemble machine learning techniques with EEG signals," *Electronics*, vol. 10, no. 13, p. 1531, Jun. 2021.
- [52] E. Urtnasan, E. Y. Joo, and K. H. Lee, "AI-enabled algorithm for automatic classification of sleep disorders based on single-lead electrocardiogram," *Diagnostics*, vol. 11, no. 11, p. 2054, Nov. 2021. [Online]. Available: <https://www.mdpi.com/2075-4418/11/11/2054>
- [53] S. Xu, O. Faust, S. Seoni, S. Chakraborty, P. D. Barua, H. W. Loh, H. Elphick, F. Molinari, and U. R. Acharya, "A review of automated sleep disorder detection," *Comput. Biol. Med.*, vol. 150, Nov. 2022, Art. no. 106100.
- [54] O. Faust, Y. Hagiwara, T. J. Hong, O. S. Lih, and U. R. Acharya, "Deep learning for healthcare applications based on physiological signals: A review," *Comput. Methods Programs Biomed.*, vol. 161, pp. 1–13, Jul. 2018. [Online]. Available: <https://www.sciencedirect.com/science/article/pii/S0169260718301226>
- [55] O. Faust, H. Razaghi, R. Barika, E. J. Ciaccio, and U. R. Acharya, "A review of automated sleep stage scoring based on physiological signals for the new millennia," *Comput. Methods Programs Biomed.*, vol. 176, pp. 81–91, Jul. 2019. [Online]. Available: <https://www.sciencedirect.com/science/article/pii/S0169260718313865>
- [56] B. Mirza, W. Wang, J. Wang, H. Choi, N. C. Chung, and P. Ping, "Machine learning and integrative analysis of biomedical big data," *Genes*, vol. 10, no. 2, p. 87, Jan. 2019. [Online]. Available: <https://www.mdpi.com/2073-4425/10/2/87>



ADITYA WADICHAR received the B.Tech. degree in electronics and communication engineering from the Visvesvaraya National Institute of Technology, Nagpur, India, in 2022. His expertise lies biomedical signal processing, deep learning, NLP, and artificial intelligence.



SHRUTI MURARKA graduate in electronics and communication engineering from the Visvesvaraya National Institute of Technology, India, in 2022. Her professional focus centers on the dynamic intersection of biomedical signal processing, deep learning, and artificial intelligence, reflecting the dedication to advancing cutting-edge technology. With a relentless passion for innovation, her contributions hold immense promise for the fields she explores, making valuable contributor to the journal and the wider scientific community.



DHRUVI SHAH received the B.Tech. degree in electronics and communication engineering from the Visvesvaraya National Institute of Technology, in 2022. She is a dedicated professional with a strong academic background in Electronics and Communication. With a blend of technical expertise and a commitment to pushing the boundaries of computer vision, she is poised to make significant contributions to the world of research and technology. Her primary research interest includes revolve around computer vision, where she passionately explores innovative approaches to advance the field.



ANKIT BHURANE received the B.E. degree in electronics and communication from Sant Gadge Baba Amravati University, in 2008, the M.Tech. degree in electronics from SGGGS Nanded, in 2011, and the Ph.D. degree from the Indian Institute of Technology Bombay (IITB), in 2016. He has more than eight years of experience in teaching undergraduate and postgraduate courses at various institutes of national importance, such as the Indian Institute of Information Technology and the National Institute of Technology. He has published several papers in various international conferences and journals. Furthermore, he has two Indian Patent Granted, and three filed with IPR Office, India. His research interests include embedded systems, biomedical signal processing, scalable video coding, and green communication. He has been an active reviewer for reputed IEEE conferences and Elsevier journals.



MANISH SHARMA received the Ph.D. degree in electrical engineering from IIT Bombay. From 2016 to 2017, he was a Postdoctoral Fellow with IIT Indore. He is currently a Faculty Member with the Department of Electrical and Computer Science Engineering, Institute of Infrastructure, Technology, Research and Management (IITRAM), Ahmedabad, India, an autonomous university established by the Government of Gujarat. He has more than 80 publications in reputed journals and conferences, of which an H-index of 36 and an i-10 index of 56 (per Google Scholar, August 2023). His research interests include machine learning, healthcare data analytics, signal processing, and their applications. He received the “Excellence in the Ph.D. Research Work” (Best Ph.D. Thesis) Award for outstanding research contributions from IIT, Bombay, in 2015. His research paper received the Honors Paper Award in recognition of outstanding work published in the SCI-indexed journal *Computers in Biology*, in 2018. In June 2018, he received the “ERCIM” Alain Bensoussan Fellowship of the European Union for research from the Norwegian University of Science and Technology (NTNU), Norway. He has been listed in the world’s top 2% of scientists in a study by Stanford University, USA, for three consecutive years (2019, 2020, and 2021).



HASAN S. MIR (Senior Member, IEEE) received the B.S. (cum laude), M.S., and Ph.D. degrees in electrical engineering from the University of Washington, Seattle, WA, USA, in 2000, 2001, and 2005, respectively. From 2005 to 2009, he was a member of the Technical Staff with the Air Defense Technology Group, MIT Lincoln Laboratory, Lexington, MA, USA, where he was involved in several projects related to airborne and maritime radar systems. Since 2009, he has been with the Department of Electrical Engineering, American University of Sharjah, where he is currently a Professor. His research interests include radar signal processing and adaptive beamforming. He serves as a Senior Editor for the IEEE TRANSACTIONS ON AEROSPACE AND ELECTRONIC SYSTEMS and an Associate Editor for IEEE ACCESS, *IET Microwaves, Antenna and Propagation*, and *IET Signal Processing*.



U. RAJENDRA ACHARYA (Senior Member, IEEE) received the Ph.D., D.Eng., and D.Sc. degrees. He is currently a Professor with the University of Southern Queensland, Australia; a Distinguished Professor with the International Research Organization for Advanced Science and Technology, Kumamoto University, Japan; and an Adjunct Professor with the University of Malaya, Malaysia, and Asia University, Taiwan. His funded research has accrued cumulative grants exceeding six million Singapore dollars. He has authored more than 600 publications, including 550 in refereed international journals, 42 in international conference proceedings, and 17 books. He has received more than 72000 citations on Google Scholar (with an H-index of 134). His research interests include biomedical imaging and signal processing, data mining, and visualization, and applications of biophysics for better healthcare design and delivery. He has been ranked in the top 1% of the highly cited researchers for the last seven consecutive years (2016–2022) in computer science, according to the Essential Science Indicators of Thomson. He is on the editorial boards of many journals and has served as the guest editor on several AI-related issues.

...